

## Intraplate stresses due to crustal heterogeneities along the Nagaur–Jhalawar transect, northwestern India

A. Manglik\*, Tanvi Arora, S. Thiagarajan and Ayan Mallick

National Geophysical Research Institute  
(Council of Scientific and Industrial Research), Uppal Road,  
Hyderabad 500 606, India

**The NW–SE trending Nagaur–Jhalawar deep crustal seismic profile transect across the Aravalli–Delhi Fold Belt to delineate the crustal structure and infer about the tectonics of this region. Seismic and gravity analyses of this profile revealed a complex tectonic structure in the central part of the profile, including the presence of a crustal-scale thrust with surface exposure near Jahazpur and a domal structure beneath the Delhi Fold Belt (DFB). In the present work, we have estimated elastic intraplate stresses due to density heterogeneities and mechanical property variations, induced by such a complex crustal structure, under the plane strain approximation for a range of elastic parameters using finite element method. The results indicate that the mechanical properties of the domal structure beneath the DFB and the lower crust control the level of stress concentration in the upper crust. A significant enhancement in the magnitude of the shear stress in the central part of the profile was obtained for the models in which either the domal structure or the lower crust was mechanically weak in comparison to the models having mechanically strong domal structure and lower crust.**

**Keywords:** Continental crust, elastic intraplate stresses, Nagaur–Jhalawar profile, plane strain.

THE Aravalli–Delhi Fold Belt (ADFB) represents one of the oldest nuclei related to the evolution of the Indian continental crust<sup>1</sup>. It is considered as a chain of relic mountains extending in the NE–SW direction for about 700 km and consisting of intensely folded, deformed and metamorphosed Proterozoic rocks overlying the Archaean gneissic basement<sup>2</sup>. The fold belt is bounded in the NW by neo-Proterozoic Marwar Basin and in the SE by meso-neo-Proterozoic Vindhyan Basin (Figure 1). Aravalli sequences and the Vindhyan basin are separated by the Great Boundary Fault. This NE–SW trending fault zone with a width of 10–20 km extends up to the Moho and probably deeper<sup>3,4</sup>. The Marwar Basin (MB), the youngest Proterozoic sequence, consists of flat, undeformed clay evaporate sequences, sandstones and siltstones overlying the Erinpura granites and the Malani igneous suite. This

intracontinental sedimentary basin extends in the NE–SW direction with a slight westerly tilt.

A 400-km-long NW–SE trending deep crustal seismic profile, the Nagaur–Jhalawar transect, was shot across ADFB (Figure 1) to delineate the crustal structure and infer about the tectonics of this region<sup>5</sup>. The transect starts from Nagaur in the neo-Proterozoic MB, cuts across the palaeo-meso-Proterozoic Aravalli Fold Belt (AFB) and Delhi Fold Belts (DFB), Achaean Sandmata Complex, Mangalwar Complex, Hindoli Group, and ends in the meso-neo-Proterozoic Vindhyan Basin at Kunjer. Further geophysical investigations incorporating magnetotelluric<sup>6</sup> and gravity studies<sup>5,7,8</sup> were carried out along this transect to develop models of tectonic evolution of the region. These studies revealed a complex nature of the sub-crustal structure, including the presence of a high-density intrusive forming a dome-shaped structure in the mid-to-lower crust beneath the DFB.

The complex nature of the crustal structure with significant lateral density variations is expected to generate a large concentration of stresses in the crust. Seismological data (magnitude  $\geq 4.0$ ) since 1849 (Table 1, Figure 1; <http://www.usgs.gov>) on the other hand, reveal that this region is not seismically very active. In the present work, we have analysed elastic intraplate stresses which might generate in the crust due to such a complex structure for different scenarios of elastic properties of various crustal layers. Although this region has not shown a significant level of intraplate seismicity, it is worthwhile to investi-

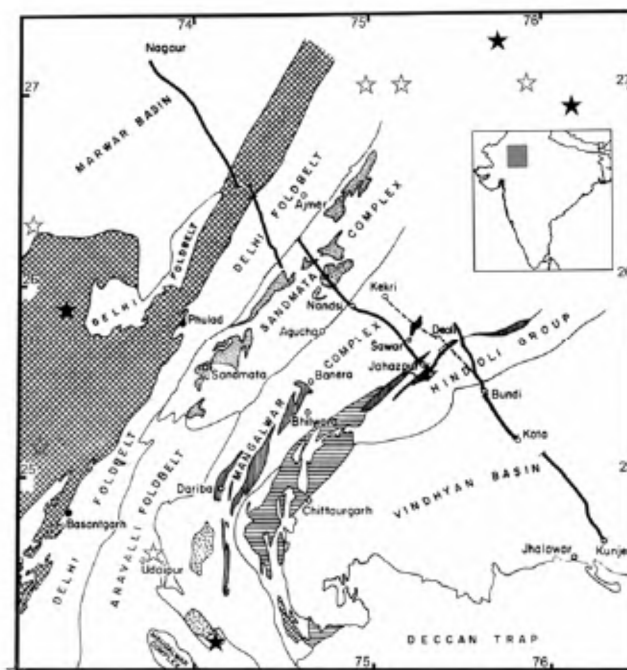


**Figure 1.** Location of the Nagaur–Jhalawar transect across the Aravalli–Delhi Fold Belt. Open and filled stars show the epicentres of historical and recent earthquakes respectively, given in Table 1. (Modified after Rajendra Prasad *et al.*<sup>7</sup>.)

\*For correspondence. (e-mail: [ajay@ngri.res.in](mailto:ajay@ngri.res.in))

**Table 1.** Earthquakes in the geographical area bounded between 24–28°N lat. and 73–77°E long., taken from the NEIC catalogue (<http://www.usgs.gov>)

Catalogue	Date	Time	Latitude (N)	Longitude (E)	Magnitude
PDE	19861102	06:16:43.67	26.53	76.90	–
PDE	19871102	09:41:29.42	25.86	73.31	–
PDE	19920530	20:17:29.96	24.14	74.12	–
PDE	20020502	14:29:45.93	27.70	75.81	4.1
PDE	20030810	11:17:54.38	27.22	75.74	4.5
PDE	20061129	05:41:14.18	27.35	76.83	4.0
PDE	20061224	22:43:26.73	26.88	76.15	4.2
INDIA	18490102	–	25.15	73.15	–
INDIA	18760703	–	24.60	73.78	–
INDIA	19001014	–	26.30	73.13	–
INDIA	19620901	22:51:30	24.00	73.00	5.0
INDIA	19670511	–	27.00	75.90	4.3
INDIA	19690820	–	27.00	75.00	4.5
INDIA	19730626	–	27.00	75.20	–

gate the stress state of the region to understand the role of the dome-shaped structure beneath the DFB in inducing local stresses. We have used finite element method<sup>9,10</sup> to compute elastic stresses due to variations in the mechanical properties and density.

The geological history of the northwestern part of the Indian craton covers a wide time span of 3.5–0.5 Ga, with the oldest cratonic nuclei of the region represented by Bhilwara Supergroup constituted of the Sandmata and the Mangalwar complexes, and the Hindoli Group<sup>11</sup>. The Sandmata complex mainly comprises of lower crustal granulite facies rocks<sup>12</sup>, whereas the Mangalwar Complex with metavolcanics and metasediments is regarded as an old granite–greenstone belt with amphibolite facies metamorphism<sup>2</sup>. The Hindoli Group of rocks consists of volcano-sedimentary sequences consisting of both mafic and felsic volcanics.

The most conspicuous geological and physiographical feature of the region is the NE–SW trending, 700 km long ADFB consisting of intensely folded, deformed and metamorphosed rocks. The lower to middle Proterozoic AFB and middle to upper Proterozoic DFB Supergroup of rocks, underlain by the Archaen Banded Gneissic Complex (BGC) as basement, constitute the Aravalli–Delhi Mobile Belt. The DFB consists of intensely folded and deformed rocks exhibiting polyphase metamorphism and represents a collision zone formed as a result of the westward movement of the Archaen craton and its collision with another craton in the west, causing eastward underthrusting of oceanic crust<sup>2</sup>. It is a highly disturbed tectonic zone comprising of a system of half grabens and horsts, with over 10 km thick volcano-sedimentary sequences. The DFB is also believed to have undergone another episode of tectono-magmatic deformation at the end of the Proterozoic resulting in an igneous suite and intrusive granites<sup>13</sup>.

The NW–SE trending Nagaur–Jhalawar deep crustal seismic profile (Figure 1) was shot across the ADFB per-

pendicular to its strike direction to delineate the crustal structure and infer about the tectonics of this region. It passes through the main geological formations of the area, including Marwar Sediments, the DFB, the Sandmata Complex, the Mangalwar Complex, the Hindoli Group and the Vindhyan Basin<sup>14</sup>. The Upper Proterozoic Vindhyan and Marwar Supergroup of rocks occur at the SE and NW parts respectively, of the transect. The Vindhyan are composed of undeformed and unmetamorphosed rocks comprising conglomerates, sandstones, shales and limestones. The MB consists mainly of dolomite, sandstone, siltstone, limestone, chert and clay, and overlies the Malani Igneous Suite.

The crustal structure of the AFB and DFB, and the surrounding Vindhyan and Marwar basins has been delineated from deep crustal seismic, magnetotelluric (MT), and gravity data along the Nagaur–Jhalawar transect. Initial deep crustal seismic results<sup>5</sup> revealed the presence of a major NW-dipping thrust fault, reaching up to the Moho, with surface exposure near Jahazpur (Jahazpur thrust). A strong upward convex reflection was also identified beneath the DFB. However, the Moho reflections beneath the DFB could not be identified. In the absence of velocity–depth section, Tewari *et al.*<sup>5</sup> and Rajendra Prasad *et al.*<sup>7</sup> interpreted the two-way travel time (TWT) seismic data in conjunction with the Bouguer gravity anomaly data along the profile and obtained an integrated model of the crustal structure (Figure 2). The high Bouguer anomaly, flanked on either side by gravity lows, observed in the central part of the profile extends in the NE–SW direction all along the ADFB<sup>15,16</sup>. This model reveals mainly a three-layered crust for most part of the profile, except for the central portion where a high-density intrusive, reaching up to the middle crust along the thrust, has been identified. Satyavani *et al.*<sup>17</sup> however, delineated a four-layered model of the crust for the northwestern Nagaur–Rian sector of the Nagaur–Jhalawar profile, the fourth layer being a low-velocity layer sandwiched

**Table 2.** Elastic properties assigned to various zones shown in Figure 2 for different models. Density values were taken from Tewari *et al.*<sup>5</sup>. For velocity values, <sup>a</sup>represents Tewari *et al.*<sup>5</sup> and <sup>b</sup>Satyavani *et al.*<sup>17</sup>. Seismic velocity for the Vindhyan was assumed

Patch no.	Model no.	$E$ ( $\times 10^{10}$ Pa)	$\nu$	$\rho$ (kg/m <sup>3</sup> )	$V_p$ (km/s)
S1 (asthenosphere)	AD01–AD06	0.1	0.499	3400	—
S2 (lower lithosphere)	AD01–AD06	0.8	0.46	3400	—
S3 (sub-Moho lithosphere)	AD02, AD06	18.0	0.25	3350	8.4 <sup>a</sup> , 8.0–8.1 <sup>b</sup>
S3 (sub-Moho lithosphere)	AD03, AD04	6.0	0.35	3350	8.4 <sup>a</sup> , 8.0–8.1 <sup>b</sup>
S3 (sub-Moho lithosphere)	AD05	1.0	0.35	3350	8.4 <sup>a</sup> , 8.0–8.1 <sup>b</sup>
S4, S6 (lower crust)	AD04, AD05, AD06	8.0	0.25	2900	7.2 <sup>b</sup>
S4, S6 (lower crust)	AD02	3.0	0.35	2900	7.2 <sup>b</sup>
S4, S6 (lower crust)	AD03	1.0	0.25	2900	7.2 <sup>b</sup>
S5, S9 (middle crust)	AD02–AD06	2.0	0.25	2750	6.6 <sup>a</sup> , 6.3–6.5 <sup>b</sup>
S7, S8 (domal structure)	AD02, AD03, AD04	12.0	0.25	3100	7.3 <sup>a</sup>
S7, S8 (domal structure)	AD05, AD06	1.0	0.35	3100	7.3 <sup>a</sup>
S10 (upper crust)	AD02–AD06	6.5	0.25	2670	5.75 <sup>a</sup> , 5.5 <sup>b</sup>
S11 (Vindhyan)	AD02–AD06	2.0	0.25	2400	5.0–5.5

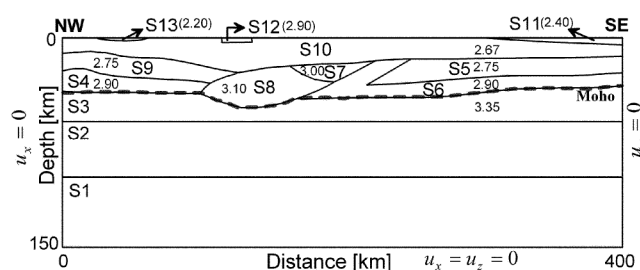


**Figure 2.** Simplified crustal structure along the Nagaur–Jhalawar profile, derived from seismic TWT data and gravity modelling<sup>7</sup>, used for finite element discretization along with boundary conditions at the left, right and bottom boundaries. The finite element model has been constructed from 11 patches marked as S1–S11. Material properties of these patches are given in Table 2. Patches S12 and S13 have not been included in the modelling.

between the mid-crustal and lower-crustal layers. The thickness of the Vindhyan sediments reaches to 4–5 km in the southeastern end of the profile. More recently, Vijaya Rao *et al.*<sup>14</sup> carried out reflectivity analysis and suggested that the upper crust is poorly reflective with some horizontal and dipping reflections, whereas the lower crustal reflectivity varies considerably all along the profile. They also correlated the Jahazpur thrust, seen in the seismic section, with the electrical conductor mapped by MT studies<sup>6</sup>. This conductor, having electrical resistivity of 50  $\Omega$ m, starts at 3 km depth near Jahazpur and extends at least up to 25 km depth.

We have taken the model of the crustal structure along the Nagaur–Jhalawar profile proposed by Rajendra Prasad *et al.*<sup>7</sup>, based on seismic TWT data and gravity modelling to numerically model elastic stresses due to crustal density heterogeneities and mechanical property variations. This crustal model provides the structure up to the Moho. Following Manglik *et al.*<sup>18</sup>, we have included a sub-Moho layer up to 60 km depth and two additional artificial layers with weak elastic parameters (Table 2) below 60 km

to the depth of 150 km, to simulate the effect of lower lithosphere and asthenosphere. This also helps in avoiding any artefacts of the no-displacement bottom boundary condition on the estimates of stresses at the Moho. The base of these layers has been assumed to be horizontal in the absence of the lithospheric structure. The model thus generated for the finite element model analysis is shown in Figure 2.

The above model has been sub-divided into 13 patches numbered S1–S13 in Figure 2. We have ignored two shallow features, having densities of 2.9 (S12) and 2.2 g/cm<sup>3</sup> (S13) respectively, in the present analysis as these were too small to have any significant influence on the regional stress estimates. Besides, seismic results have not provided any evidence of a near-surface high-density body in the region<sup>5</sup>. The finite element model consisting of 11 patches (S1–S11) has been discretized into 5176 plane strain four-node quadrilateral elements and 5330 nodes. Since the Nagaur–Jhalawar profile is oriented orthogonal to the general strike of the ADFB, plane strain approximation is valid for the stress analysis. Elastic material parameters for every patch were selected based on seismic  $P$ -wave velocity, density and depth of various layers (Table 2).

We have estimated Young's modulus from seismic  $P$ -wave velocity and density values using the seismic velocity and density values reported in the literature and the following relationship<sup>19</sup>:

$$E = \rho V_p^2 \frac{(1+\nu)(1-2\nu)}{3\nu}, \quad (1)$$

where,  $E$ ,  $\nu$ ,  $\rho$ ,  $V_p$  are the Young's modulus, Poisson's ratio, density and seismic  $P$ -wave velocity respectively. For the values of  $\rho$  and  $V_p$  of crustal rocks of this region,  $E$  varies in the range of 4–12  $\times 10^{10}$  Pa. However, we have considered slightly lower values of  $E$  for the mid- and lower

crust to account for the rheological weakening of these layers due to the increase in temperature<sup>20,21</sup>. The value of  $E$  has also been lowered by a factor of two for the Vindhyan rocks, as it falls in the range  $1\text{--}3 \times 10^{10}$  Pa for shale and sandstone<sup>22</sup>. The sub-Moho layer is the strongest with  $E = 18 \times 10^{10}$  Pa for the estimated velocity and density of 8.0 km/s and 3.35 g/cm<sup>3</sup> respectively. The material properties thus obtained are given in Table 2. The values of  $E$  estimated by this approach were in good agreement with the value of  $7 \times 10^{10}$  Pa used by Coblenz *et al.*<sup>23</sup> and Reynolds *et al.*<sup>24</sup> to model the stress state of continental Australia.

In all the models presented in the following, we assume that there is no horizontal displacement ( $u_x = 0$ ) across the left and right boundaries and the bottom boundary is a no-displacement boundary ( $u_x = u_z = 0$ ). We have not incorporated the effect of topographic load in our present model. The only load applied in the model was the internal gravity load due to the crustal density variations. We have analysed various cases of internal gravity load. Computations have been carried out using the FEM package UWay<sup>9,10</sup>. This package has options for numerical estimation of stress-strain state and mechanical behaviour of the soil and consolidated rocks, homogeneous and heterogeneous media, and composite materials.

We have computed various model cases to analyse the level of stress concentration due to lateral variations in the crustal structure of the ADFB and to explore the possibility of a suitable model case which yields the least stress concentration to corroborate with the low level of seismicity in this region. Numerical results for different cases are discussed below.

In the first model (AD01), we have analysed the effect of only density heterogeneities on stress generation. Here, material parameters of all the layers, except the two bottom layers S1 and S2, treated as rheologically weak layers, have been fixed at  $E = 6.5 \times 10^{10}$  Pa and  $\nu = 0.25$ . The computed maximum shear stress ( $\tau$ ) for this gravity loading case is shown in Figure 3a. Results below the depth of 60 km are not shown as these correspond to fictitious layers. Crustal structure is also superimposed. For this case,  $\tau$  increases with depth with the maximum value of more than 600 MPa at a depth of 55–58 km. The results do not show any appreciable lateral variation in  $\tau$  due only to the density variations.

In the next model (AD02), we have prescribed the elastic parameters to various layers as given in Table 2. In this model case, the lower crust (S4, S6) was assumed to be rheologically weaker than the underlying sub-Moho mantle (S3). Therefore, a reduced value of  $E = 3.0 \times 10^{10}$  Pa was assumed for this layer to represent a rheologically weak lower crust. This model has been selected to represent a case similar to the rheological stratification of a typical continental lithosphere in which a weak, ductile lower crust overlies a strong, brittle upper mantle<sup>20,25</sup>. In this case, the domal structure (S7, S8) has

also been considered as a mechanically strong body based on its density and seismic velocity. Tewari *et al.*<sup>5</sup> inferred the poor reflectivity in this region to the presence of dry granulite which can be considered as rheologically strong. Although patches S7 and S8 have been demarcated<sup>3,7</sup> as two different bodies having a density difference of 0.1 g/cm, we have considered the same elastic properties for these two patches. The distribution of  $\tau$  for this case (Figure 3b), yields a significant lateral variation in the central region of the profile demarcated by the presence of a domal structure having high density. Although the concentration of maximum  $\tau$  occurred in the sub-Moho layer, the shear stress state of the crust was significantly perturbed within the central region. The model also shows a localization of  $\tau$  in the near-surface region at a profile distance of 120–140 km from its NW end corresponding to the DFB.

In the next model case (AD03), we have analysed the effect of mechanically strong domal structure ( $E = 12.0 \times 10^{10}$  Pa) buried in a mechanically weak lower crust ( $E = 1.0 \times 10^{10}$  Pa) and relatively weak sub-Moho mantle ( $E = 6.0 \times 10^{10}$  Pa) on stress generation. For this case, the stress state seems to be highly perturbed with the largest shear stress occurring in the sub-Moho layer beneath the domal structure (Figure 3c). An enhanced shear stress level was also obtained in the lower crust at 250 km profile distance. The shear stress in the near surface region in the DFB further increased to 160–180 MPa.

The above models have included a mechanically weak lower crust compared to the sub-Moho layer. We further

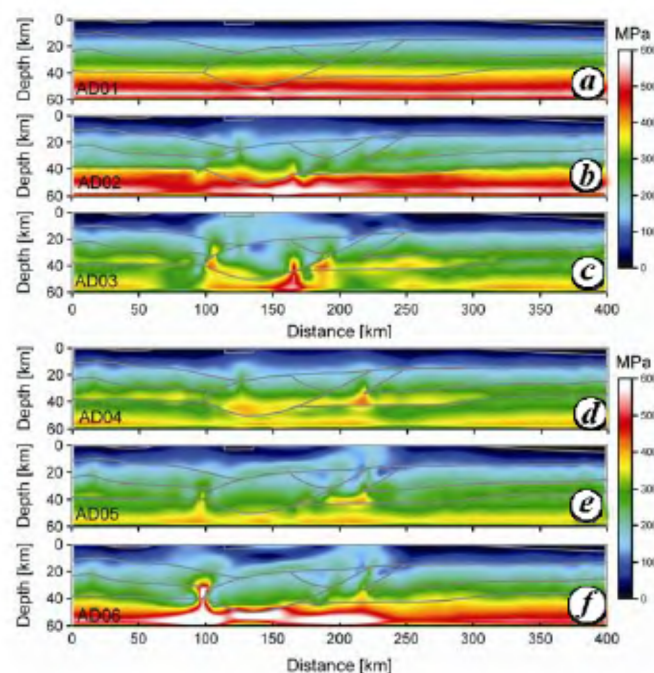


**Figure 3.** Computed maximum shear stress (MPa) for various model cases: (a) AD01, (b) AD02, (c) AD03, (d) AD04, (e) AD05 and (f) AD06.



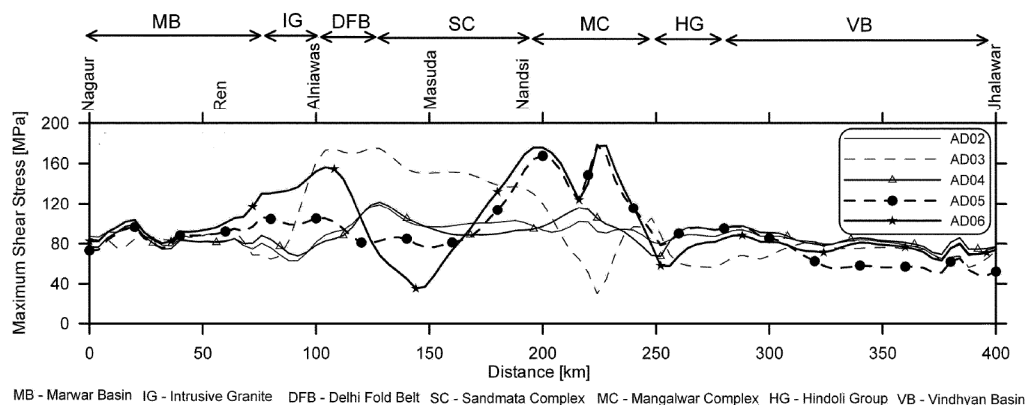


**Figure 4.** Computed maximum shear stress at 10 km depth along the profile for model cases, AD02–AD06.

analysed the effect of having a strong lower crust and weak sub-Moho, as inferred for the Jabalpur earthquake region<sup>18</sup>, on stress generation in the next set of models. Model AD04 incorporates mechanically strong lower crust with  $E = 8.0 \times 10^{10}$  Pa resting over a relatively weak sub-Moho layer with  $E = 6.0 \times 10^{10}$  Pa. These values were not significantly different, except that  $\nu$  was 0.35 in the case of the sub-Moho layer. The elastic parameters of the domal structure were kept the same as for the model AD03. For this case, the pattern of stress concentration, especially in the upper 20 km of the crust, was similar to that of AD02 (Figure 3 *d*). Nevertheless, the large stresses beneath the Moho, as obtained for AD02, get distributed in the lower crustal and sub-Moho layers in the present model. This model also shows a concentration of stresses in the lower crust at the profile distance of 220 km just beneath the sharp bend.

The next model (AD05) incorporates strong lower crust with the value of  $E$  as in the model AD04, weak sub-Moho layer ( $E = 1.0 \times 10^{10}$  Pa), and also weak domal structure ( $E = 1.0 \times 10^{10}$  Pa). This model yielded strong lateral variations in the shear stress (Figure 3 *e*) in the upper 20–25 km of the crust at the profile distance of 190–250 km. The shear stress remained less than 300 MPa in the lower crust, except in a small patch at the profile distance of 190–230 km. A change in the elastic parameter of the sub-Moho layer to  $E = 19.0 \times 10^{10}$  Pa in the above model (AD05) resulted in an increase in the magnitude of  $\tau$  to more than 600 MPa in the sub-Moho layer (model AD06, Figure 3 *f*), while the pattern of  $\tau$  in the upper crust remained largely similar to that obtained for the model AD05. A vertical zone of large  $\tau$  at 100 km profile distance now becomes more pronounced, affecting the stress state of the upper crust also.

The above results (Figure 3 *a–f*) imply that the mechanical properties of the lower crust, intrusive part of the lower crust (inclined structure east of the domal structure), sub-Moho lithosphere and domal structure have profound effect on the stress state of the ADFB region. Density heterogeneities alone are not sufficient to induce

significant lateral variations in the stresses. Since it is difficult to measure the stress level of the crust except for the upper few kilometres, we have analysed the stress state in the upper crust for various model cases considered here. A model with strong lower crust, upper mantle and domal structure only moderately increases the shear stress in the upper crust (AD02, AD04). In contrast, models having mechanically strong domal structure in contact with a weak lower crust, or weak domal structure in contact with a strong lower crust reveal a zone of increased shear stress in the upper crust.

The location of this zone of enhanced shear stress concentration shifts depending on the relative strength of the domal structure and lower crust. This can be clearly seen in Figure 4, where the distribution of the shear stress at 10 km depth is plotted along the profile. The depth of 10 km was chosen as most of the intraplate seismicity in the Indian shield region has occurred in the upper 10 km of the crust. Here, all the models show an increase in the magnitude of the shear stress in the region covered by the Intrusive Granite (IG), the DFB, Sandmata Complex (SC) and Mangalwar Complex (MC). This increase, however, is on an average about 40 MPa from the background level in the case of mechanically strong domal structure and lower crust (AD02, AD04). The increase in the shear stress becomes more pronounced with an increase of about 120 MPa from the background level in the DFB and SC regions when the lower crust is considered as mechanically weak (AD03). Maximum stress concentration was observed beneath the DFB for this model case. For the model with mechanically weak domal structure in a strong lower crust (AD05), the zone of enhanced stress concentration shifted to the MC region and it become narrower than the previous case. There was another small zone of stress increase beneath the IG. An increase in the Young's modulus of the sub-Moho layer in the above model yielded further enhancement in the stress level (AD06).

The above results show that the crustal structure along the Nagaur–Jhalawar profile, as delineated by seismic

and gravity studies, should induce significant intraplate stresses in the crust, especially in the complex tectonic zone demarcated by domal high velocity structure and intrusive body along the Jahazpur thrust. The mechanical properties of these structures influence the stress state in the shallow part of the crust and lead to stress concentration in various parts of the profile. These results, in corroboration with measured stress data when available, can help in constraining models of the crust of this region.

1. Naqvi, S. M., Divakara Rao, V. and Hari Narain, The protocontinental growth of the Indian shield and the antiquity of its rift valleys. *Precambrian Res.*, 1974, **1**, 345–398.
2. Sinha-Roy, S., Precambrian of the Aravalli mountain, Rajasthan, India. *Geol. Soc. India, Mem.*, 1988, **7**, 95–108.
3. Pascoe, H., *A Manual of Geology of India and Burma*, Govt of India Press, Calcutta, 1959, vol. 2, pp. 495–561.
4. Banerjee, A. K. and Sinha, P. N., Structure and tectonics of the Vindhyan in the eastern Rajasthan. *Misc. Publ. Geol. Surv. India*, 1981, **50**, 41–47.
5. Tewari, H. C., Dixit, M. M., Rao, N. M., Venkateswarlu, N. and Vijaya Rao, V., Crustal thickening under the Paleo/mesoproterozoic Delhi Fold Belt in NW India: evidence from deep reflection profiling. *Geophys. J. Int.*, 1997, **129**, 657–668.
6. Gokarn, S. G., Rao, C. K. and Singh, B. P., Continental Crust of NW and Central India. *Geol. Soc. India Mem.*, 1995, **31**, 373–381.
7. Rajendra Prasad, B., Tewari, H. C., Vijaya Rao, V., Dixit, M. M. and Reddy, P. R., Structure and tectonics of the Proterozoic Aravalli–Delhi fold belt in NW India from deep seismic reflection studies. *Tectonophysics*, 1998, **288**, 31–41.
8. Mishra, D. C., Singh, B., Tiwari, V. M., Gupta, S. B. and Rao, M. B. S. V., Two cases of continental collisions and related tectonics during the Proterozoic period in India – insights from gravity modelling constrained by seismic and magnetotelluric studies. *Precambrian Res.*, 2000, **99**, 1490169.
9. Vlasov, A. N., Mnushkin, M. G. and Yanovsky, Yu. G., Object-oriented Approach in Programming of Finite Element Method. In Proceedings of the Third International Conference on Advances of Computer Methods in Geotechnical and Geoenvironmental Engineering (ed. Yufin, S. A.), A. A. Balkema Publ. Co, 2000, pp. 367–372.
10. Vlasov, A. N., Yanovsky, Yu. G., Mnushkin, M. G. and Popov, A. A., Solving geomechanical problems with UWay FEM package. In *Computational Methods in Engineering and Science* (ed. Iu, V. P.), Taylor & Francis, 2004, pp. 453–461.
11. Sinha-Roy, S., Malhotra, G. and Guha, D. B., Continental crust of NW and Central India. *Geol. Soc. India, Mem.*, 1995, **31**, 63–89.
12. Sharma, R. S., Precambrian of the Aravalli mountain Rajasthan, India. *Geol. Soc. India Mem.*, 1988, **7**, 33–75.
13. Roy, A. B. (ed.), Precambrian of the Aravalli mountain, Rajasthan, India. *Geol. Soc. India Mem.*, 1988, **7**, 3–32.
14. Vijaya Rao, V., Rajendra Prasad, B., Reddy, P. R. and Tewari, H. C., Evolution of Proterozoic Aravalli Delhi Fold Belt in the northwestern Indian Shield from seismic studies. *Tectonophysics*, 2000, **327**, 109–130.
15. Reddy, A. G. B. and Ramakrishna, T. S., Precambrian of the Aravalli mountain, Rajasthan, India. *Geol. Soc. India, Mem.*, 1988, **7**, 279–284.
16. Mishra, D. C., Laxman, G., Rao, M. B. S. V. and Gupta, S. B., Continental crust of NW and Central India. *Geol. Soc. India, Mem.*, 1995, **31**, 345–352.
17. Satyavani, N., Dixit, M. M. and Reddy, P. R., Crustal velocity structure along the Nagaur–Rian sector of the Aravalli fold belt, India, using reflection data. *J. Geodyn.*, 2001, **31**, 429–443.
18. Manglik, A., Thiagarajan, S., Mikhailova, A. V. and Rebetsky, Yu., Finite element modelling of elastic intraplate stresses due to heterogeneities in crustal density and mechanical properties for the Jabalpur earthquake region, central India. *J. Earth Syst. Sci.*, 2008, **117**, 103–111.
19. Pauselli, C. and Federico, C., Elastic modelling of the Alto Tiberina normal fault (central Italy): geometry and lithological stratification influences on the local stress field. *Tectonophysics*, 2003, **374**, 99–113.
20. Manglik, A. and Singh, R. N., Rheological stratification of the Indian continental lithosphere: role of diffusion creep. *Proc. Indian Acad. Sci. (Earth Planet. Sci.)*, 1999, **108**, 15–21.
21. Manglik, A. and Singh, R. N., Thermomechanical structure of the central Indian shield: constraints from deep crustal seismicity. *Curr. Sci.*, 2002, **82**, 1151–1157.
22. Turcotte, D. L. and Schubert, G., *Geodynamics: Applications of Continuum Physics to Geological Problems*, John Wiley, New York, 1982, p. 450.
23. Coblenz, D. D., Sandiford, M., Richardson, R. M., Zhou, S. and Hillis, R., The origins of the intraplate stress field in continental Australia. *Earth Planet. Sci. Lett.*, 1995, **133**, 299–309.
24. Reynolds, S. D., Coblenz, D. D. and Hillis, R. R., Tectonic forces controlling the regional intraplate stress field in continental Australia: Results from new finite element modelling. *J. Geophys. Res.*, 2002, **107**, 2131.
25. Manglik, A. and Singh, R. N., Rheology of Indian continental crust and upper mantle. *Proc. Indian Acad. Sci. (Earth Planet. Sci.)*, 1991, **100**, 389–398.

**ACKNOWLEDGEMENTS.** This work was supported by the Department of Science and Technology, India, and Russian Academy of Sciences, Russia, under the framework of the Indo-Russian programme of collaboration (ILTP). We are grateful to the Area Chairmen of ILTP (Seismology), and the Director, NGRI, Hyderabad, and Director General, IPE, Moscow, for support. We also thank Dr Yu Rebetsky for help and for providing access to the FEM code and the anonymous reviewers for useful suggestions.

Received 14 May 2008; revised accepted 13 January 2009

## A process for making slow-release phosphate fertilizer from low-grade rock phosphate and siliceous tailings by fusion with serpentinite

**Pushpendra Ranawat\*, Kosanam Mohan Kumar and Navin K. Sharma**

Department of Geology, Mohanlal Sukhadia University, Udaipur 313 001, India

**Worldwide demand of phosphate fertilizer is met essentially from phosphatic rocks. India imports most of its requirements and produces a small portion through froth flotation of Precambrian stromatolitic rock phosphate. Increasing population and consequent increase**

\*For correspondence. (e-mail: psranawat@yahoo.com)